

# Actuation Mechanisms Used in MRI-Compatible Robotic Surgeries: A Review

<sup>[1]</sup> Sean How, <sup>[2]</sup> Majid Roshanfar, <sup>[3]</sup> Javad Dargahi

<sup>[1]</sup> <sup>[2]</sup> <sup>[3]</sup> Department of Mechanical Engineering, Concordia University, Montreal, Canada  
Corresponding Author Email: <sup>[1]</sup> seanhow@encs.concordia.ca, <sup>[2]</sup> m\_roshan@encs.concordia.ca, <sup>[3]</sup> dargahi@encs.concordia.ca

**Abstract**— There has been increasing use of robotic surgery over the years, as it has evolved as an improvement over minimally invasive surgery (MIS), where a surgeon can use a tele-manipulator to operate on a patient. Magnetic resonance imaging (MRI) has become the leading form of image acquisition due to its ability to produce high resolution images during robotically assisted MIS. However, the MRI scanner places conditions on the robots that allow only certain compatible actuation methods used in the robotic system to negate large interference that hinders the image quality. The current review focused on the four main MRI-compatible actuation mechanisms: hydraulic, pneumatic, piezoelectric, and shape memory alloy. This review mainly discussed signal-to-noise ratio (SNR) reduction, performance, and limitations from the recent publications on MRI-compatible robotic surgeries. Favorable MRI compatibility with low SNR reduction, performance, and simple implementation was observed to be the most important characteristics of a proper actuation mechanism for MRI robotic surgeries. After reviewing each approach, it was concluded that shape memory alloy, despite having a form of limitation, demonstrated to be more favorable compared to other actuation methods because of factors such as low cost, negligible SNR reduction, and high-power output for medical interventions.

**Index Terms**—Robotic surgery, magnetic resonance imaging, actuation mechanism, minimally invasive surgery, SMA.

## I. INTRODUCTION

In the last two decades, minimally invasive surgery (MIS) has gained popularity as an alternative method of performing medical procedures, in which surgical instruments are inserted through a small incision to perform the operation. Compared to traditional surgery methods, MIS has several advantages, including reduced pain, fewer post-operative complications, less permanent scarring, and shorter hospital stays [1], [2]. A clear image of the surgical site in real-time is essential for robot-assisted surgeries, which allows surgeons to have a complete view and control over the surgical site. An effective real-time imaging modality that is used in medical surgeries is magnetic resonance imaging (MRI). MRI is an imaging technique that uses nonionizing radiation to create a magnetic field to produce high-contrast images without the use of harmful ionizing radiation from x-rays and computed tomography (CT) [3], [4]. Compared to high-quality vision systems used in robot-assisted surgeries, MRI scans provide surgeons with the ability to distinguish between healthy and affected tissues through these high-contrast images. This increases the chances of success during critical surgeries that require clear imaging, such as tumor removal. Surgeons will be able to effectively distinguish between healthy and affected tissues in order to minimize any potential damage to critical organs during the operation [5].

MRI-compatible surgical robots can assist surgeons during surgical operations by providing real-time images to guide them. Li et al. [6] have provided Fig. 1, which is an overview of a clinical workflow that summarizes a typical surgical operation using MR imagery. This figure illustrates the

workflow comparison between conventional stereotactic surgery that uses imaging methods such as CT, and the MRI-assisted approach to highlight the simplified procedure using iMRI-guided robots with respect to potential errors and surgical time. Procedural time is estimated to significantly decrease due to real-time image guidance eliminating the need for lengthy procedures such as image fusion and patient registration after CT scans.

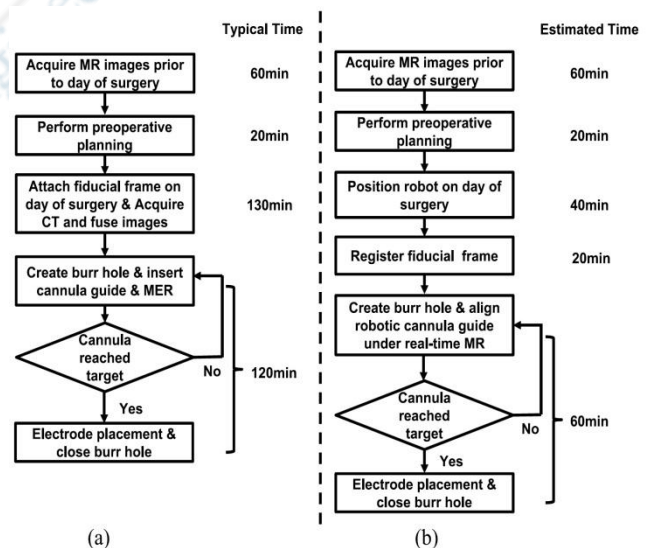


**Figure 1.** Comparison between (a) workflow of conventional stereotactic neurosurgery and (b) workflow of MRI-guided/robot-assisted stereotactic neurosurgery [6].

In spite of the advantages of robotic surgery over traditional methods, developing an MRI-compatible surgical

robot can be a challenging undertaking due to the material restrictions imposed by an MRI scanner. The robotic system needs to be electromagnetically (EM) decoupled, where it is composed of materials that exhibit non-electromagnetic and non-ferrous properties to ensure that there will not be any interference with the magnetic field of the scanner.

In addition, the narrow bore of the MRI places dimensional restrictions on the robot so that they would need to be designed small enough to work within confined spaces while not disturbing the patient lying inside the bore. Therefore, the robot needs to be extensively tested inside an MRI environment in order to ensure that it is capable of performing normally while ensuring that there is no reduction in image quality or appearance of imaging artifacts. Surgical robots that meet these criteria are specified by the FDA as “MR-safe,” while “MR-conditional” describes robotic systems that are safe to operate at a certain distance away from the scanner under specific conditions where it will not cause EM interference [7]. Not only does this limit all parts of the robot to be MRI-compatible, but also the methods of actuation for manipulating the surgical tools at certain speeds and directions. Most strong mechatronic components cannot be used, thus lowering the overall potential power of the system. MRI-compatible actuation methods include hydraulic [8], pneumatic [9], piezoelectric [10], and shape memory alloy (SMA) actuators [11].

Several MIS robots have been developed to overcome these design obstacles over the past twenty years [12]-[15]. Guo et al. [16] designed a hydraulic driving iMRI-guided robot for a 4-DoF pneumatic robot for MRI-guided prostate biopsy [17]. Su et al. designed a piezoelectrically-actuated 6-DoF MRI-guided robot with a needle driver for prostate brachytherapy [18]. Taylor et al. created an SMA origami joint actuator tailored towards MRI-guided endoscopic surgery [19]. Although robotic systems are composed of MRI-compatible materials, during initial research, actuators such as hydraulic and pneumatic have been documented to cause problems such as fuel leakage, high maintenance, and considerable time delay [20]. Piezoelectric actuators also have issues with deteriorating image quality and creating artifacts when placed near the MRI scanner [21]. SMA actuators, despite their low cost, silent operation, and high actuation force, experience long actuation speed due to natural cooling between different phase structures [22].

This paper reviews recent publications of different actuating mechanisms in order to draw comparisons between these methods used in state-of-the-art MRI-compatible surgical robots. The review paper is divided into four main sections. Section I introduces the concept of robotic surgery with real-time MRI-imagery with the different capable actuation systems and defines the necessary methodology that is discussed throughout the paper. Section II describes the method of research for the publications reviewed in this paper. Section III discusses the latest actuation methods for

recently developed MRI-compatible surgical robots and their overall performance. Section IV concludes on the topic discussed and the future of actuation methods in MRI robotic surgeries.

## II. RESEARCH METHOD

This review analyzes recent developments in actuating methods for surgical robots and draws a comparison between them based on parameters such as signal-to-noise ratio (SNR) and their relevant measured performance in an MR environment. SNR is an important measure used in this study, as different actuation methods suffer from a reduction in image quality, which is essential to maintain high-quality imaging during MIS. Articles were obtained from online databases such as IEEE Xplore, Google Scholar, and PubMed, and were manually screened for eligibility. The review was limited to articles published from years 2017 to 2022. For this review, Fig. 2 was created in order to display the relevant keywords used to obtain the publications discussed later. The data reviewed in these examples will be evaluated on the given SNR values that is based on the guidelines from the National Electrical Manufacturers Association (NEMA) [23]. Thus, any research articles that do not adhere to the standards set by NEMA, or present qualitative evaluations of MRI compatibility instead of quantitative SNR figures, are excluded from this review. The following section reviews two recent articles for each actuation method. The results from the four actuation methods discussed will then be compared in order to analyze all of their strengths and weaknesses.

### Actuation Mechanism in Medical Interventions

“Hydraulic” OR “Pneumatic” OR “Piezoelectric” OR  
“Shape memory alloy ”

AND

“Magnetic resonance imaging” OR “MR-compatible”

AND

“Robot” OR “Robotic surgery” OR “Robot-assisted”

AND

“Signal-to-noise ratio”

**Figure 2.** Keyword string method for current literature review.

## III. ACTUATION MECHANISMS IN MRI-GUIDED MEDICAL INTERVENTIONS

Robot-assisted surgeries have evolved over the years to handle more advanced medical procedures [24]-[30]. This emphasizes the importance of an actuating system that allows

for precise and accurate maneuvers of the robot's end effector during a surgical procedure. Currently, there are four main types of MRI-compatible actuating systems.

### A. Hydraulic actuators

Hydraulic actuation is one of the most general methods of generating mechanical motion [31]. It is typically accomplished through the use of hydraulic fluids, such as oil or water, to drive a piston located inside the hydraulic cylinder. The potential for high power to weight ratio makes hydraulic actuation an acceptable method to use for surgical robotic manipulators. However, it has been noted to be held back by certain limitations that have significant effects on performance and safety, which will be discussed below.

In 2018, Lee et al. [32] designed a hydraulically actuated robotic manipulator for intra-cardiac catheterization. This design presents a master-slave hydraulic transmission that uses master electric dc motors located in the control room to avoid EM interference. Hydraulic fluid is transmitted through the 1 m long hydraulic pipelines into the slave catheter robot platform in the MRI room to control actuation of the catheter. Their system was able to output a torque of  $1.47 N \times m$ , which corresponds to the master-slave actuator lifting 3 kg at a velocity of 10.01 cm/s. The slave robotic manipulator was evaluated inside a 1.5 T MRI and displayed less than 2% reduction in SNR with no visible image artifacts when under certain conditions in the scanner. Despite using stiff pipelines to maintain high precision output, the slave actuation unit suffers from slight hysteresis, where it is lagging behind the master input unit that is caused by the backlash between the motor gears. Hysteresis slightly increases with the preloaded pressure in the fluid pipelines due to the increase in static friction between the gears in the master unit. Also, the long distance of the hydraulic transmission in the flexible pipelines causes time delay.

Dong et al. [33] designed an MRI-guided robotic catheterization platform that uses a three-cylinder hydraulic motor for actuation. This system is designed for electrophysiology (EP) catheterization for cardiovascular surgery that requires responsive and precise maneuvers of the medical instruments. Long hydro-static transmission pipelines connect both sides of the master-slave device that is driven by the hydraulic motor, producing continuous bidirectional actuation of the catheter. Fig. 3 shows a portion of the setup of their robot inside the MRI scanner. At pressure of 0.1 MPa, their master-slave actuator can produce a torque of 0.49 N×m. The motor was placed inside a 1.5 T MRI scanner and concluded that the slave actuation system did not cause any electromagnetic (EM) interference, where there was close to 0% reduction in SNR.

Overall, the robot facilitates catheter insertion during surgical operations by allowing for fast insertion and can move 340 mm into the human body. However, the same trade-off between the stiffness and large diameter of the long transmission tubes, and time delay are also observed with this

robot.

Although hydraulic actuators are capable of outputting a substantial amount of actuation force with minimal loss in SNR, they have issues with certain parameters that would affect the overall performance. These include fuel leakage, hysteresis, and fluid transmission latency. Additionally, an MRI-compatible master slave actuator is not possible as the electric motor (master unit) is composed of EM components. Currently there is no MR safe hydraulic master-slave follower, so certain design tradeoffs are needed to be made in order to ensure no loss in SNR or performance [33]. As a result, robotic systems with hydraulic actuation usually have complicated setups that require a lot of maintenance.

### B. Pneumatic actuators

Pneumatic actuation is an effective method of actuation as they function similarly to hydraulic actuators, but instead use compressed air instead of fluids. Therefore, similar to hydraulic actuation, pneumatic actuation is desirable for MRI robots because of its high-performance output and minimal interference with the MRI scanner.

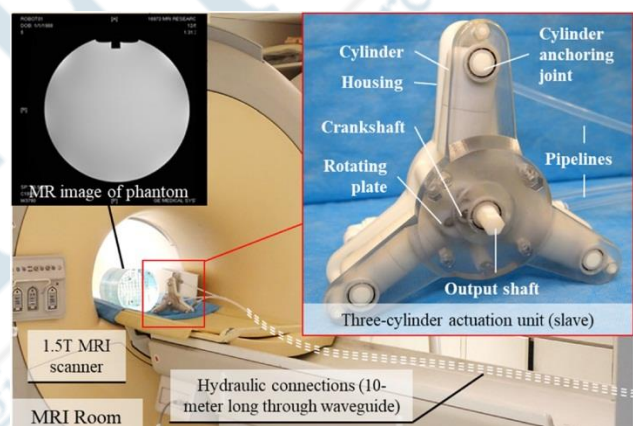


Figure 3. Hydraulic motor setup with three cylinders in a 1.5 T MRI scanner [33].

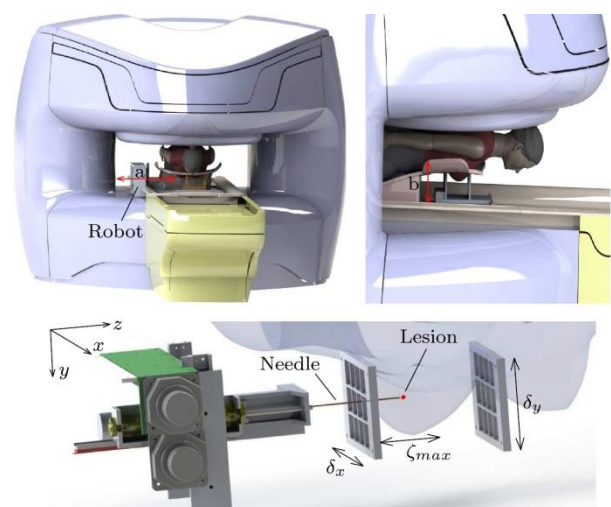


Figure 4. Setup of pneumatically actuated breast biopsy robot in open MRI bore [34].

However, they do also demonstrate certain limitations comparable to the hydraulic actuators. In 2017, Navarro-Alarcon et al. [34] created a novel robot for MRI-guided breast biopsy that is actuated by pneumatic actuators. The pneumatic cylinder transmits motion to the needle driving mechanism that consists of three linear joints for 3-DOF in order to closely simulate manual breast biopsy procedures. The system is connected by long 6 m tubes that are passed from a control room into an MRI room due to material incompatibility of the pneumatic valves that control the pressure output to the cylinder. Fig. 4 shows their experimental setup of the robot inside an open bore. MR compatibility was tested in a 0.2 T magnetic bore by scanning a phantom tissue with and without the robot. Their experimental results showed that there was no significant reduction in SNR, producing images with close to 0% SNR reduction. Their system was also tested in an MR environment by targeting a phantom inside the scanner and the mechanism demonstrated a needle positioning accuracy of  $\pm 1.5$  mm. The use of long tubes in the system and the compressible air has some effects on the insertion accuracy of the robot. In addition, there is possible air leakage and time delay due to the long and flexible tubing.

Also, Chen et al. [35] constructed a pneumatically actuated robot that uses MR-imaging for focal laser ablation of prostate cancer. Their robotic system includes a pneumatic motor and gearbox that is composed of MRI-compatible materials that is 3D printed. The system uses ten sets of pulleys that are powered through the pneumatic actuator in order to drive the needle in a two-directional motion. Their robotic system was tested inside a 3.0 T scanner and the MRI compatibility results showed a maximum of 8% SNR loss when the robot was placed in the head position of the scanner, where a bottle phantom was also placed at the scanner's isocenter. The performance of the robot was tested in a needle insertion accuracy test that demonstrated a needle insertion error of 0.9 mm along the insertion axis of the manipulator. But their robotic system suffers from error caused from complications such as gearbox backlash and friction.

Although pneumatic actuators are capable of high-power output, low SNR reduction, and are easily made of inexpensive materials that can be 3D printed, they have similar issues compared to hydraulic actuators. This includes time delay between the control unit and the actuator, friction of the gears in the motor, and possibility of air leakage due to the long tubing.

### C. Piezoelectric actuators

Piezoelectric actuators are another method of actuation in MRI-conditional robots. Due to its material compatibility issues, the robot can only safely operate in MR-conditional systems where it can operate from a safe distance or when its powered off. Therefore, conducting continuous MRI scanning while using this actuation method would introduce imaging artifacts and significantly decrease the SNR.

However, the use of piezoelectric actuation does have key advantages.

Recently, Krieger et al. [36] developed a piezoelectric actuated MRI-guided robot for prostate cancer ablation. The robotic system is composed of multiple piezoelectric motors that are located inside a housing and actuates the needle in 2-DOF. The probe is capable of being controlled through rotation and translation of the needle using several piezoelectric motors. The motor is placed more than 2 cm away from the location of the prostate in the MRI scanner in order to make sure there is not any EM interference that would result in image artifacts. The controller box and cables are shielded with radio-frequency (RF) shielding to mitigate the EM interference. Fig. 5 [36] shows their piezoelectrically actuated robot for prostate intervention. Their MRI compatibility study showed that under conditions where the controller and motor are powered inside a 3.0 T scanner, the SNR would reduce by a maximum of 80% and would only be reduced by 40-60% when they had used RF shielding. In practical cases this large reduction in SNR would not be a problem since the patient and needle are not moving during the MRI scans and the motor can be turned off during this sequence. However, slight movement by the patient would cause SNR degradation, which can accidentally happen. Lastly, the piezoelectric motors are capable of producing an output torque of 1.08 Nm when rotating the needle.

Furthermore, Shi et al. [37] developed a piezoelectric robotic system that delivers therapeutic drugs to regions affected by tumors. A controller located inside the MRI room to send inputs to the piezoelectric motor, which is used to actuate the injection of the needle during surgical procedures. The motor is shielded through aluminum foils and tapes to reduce the EM interference and SNR reduction.

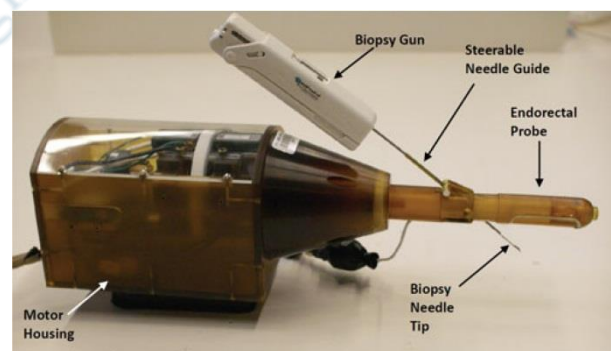


**Figure 5.** Piezoelectrically actuated robot for needle-guided prostate intervention [36].

Their MRI compatibility tests were run in a 3.0 T MRI scanner and the results showed that even with shielding, there was a substantial decrease of 21.6% in SNR. In addition, the system's positioning error was tested in experiments to be less than 0.5 mm when the moving speed was fast at 10-80 mm/s. So, the performance of their robot was very fast and optimal, yet the image quality suffered a lot when the motor was turned on even with shielding.

Therefore, even though piezoelectric actuators are capable of high precision and control as well as displaying fast response and actuation times, they are very costly, and their material composition mostly results in imaging artifacts and a large reduction in image quality. These actuators require a sophisticated shielding mechanism in order to increase MRI compatibility and lower the SNR reduction.

#### D. Shape memory alloy actuators

SMA demonstrates inherently unique properties that allow it to be an effective actuation mechanism [38]. However, the transformation from martensite and austenite phases depends on the temperature change. The material can easily be driven by generating heat; however, it must rely on the slow natural cooling process. Therefore, SMA generally has a slow response time with respect to this cycle, which mostly characterizes it as too slow for conventional surgical procedures [22]. However, SMA has been recently integrated into multiple applications for MRI robotic surgery. In 2020, Shao et al. [39] created a SMA actuated MR-conditional robotic system for brain tumor ablation. Their system is integrated into a single device that is placed in the MRI room, which greatly simplifies the workflow of the surgical procedures. It is equipped with a 2-DOF steerable end effector that is actuated by a set of two SMA springs and has a quick-connect module to change the end effector for any specific medical surgeries. The end effector is actuated left and right by heating up the opposing spring in order to revert it back to its original memorized shape. Their system incorporated fan cooling in order to cool the SMA springs, but it is not MRI compatible and will be replaced with another cooling module. Their results from MRI compatibility tests showed that there was only a 1.27% reduction in SNR. Furthermore, the robot has an actuation speed of 1.12 mm/s, which is close to the actuation speed of other neurosurgical robots that use other conventional actuation methods.

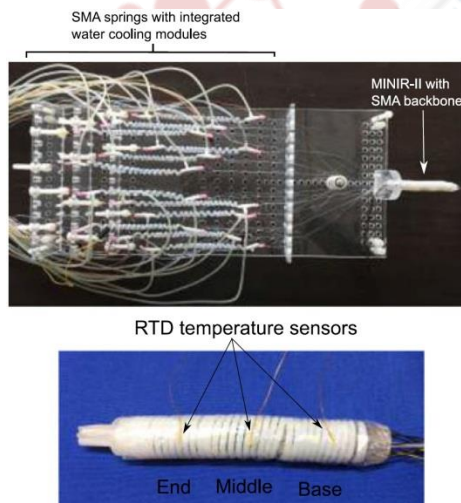


Figure 6. Setup of MINIR-II robot with actively cooled SMA springs [40].

In addition, Kim et al. [40] designed a minimally invasive neurosurgical intracranial robot (MINIR-II) for neurosurgical applications in MRI environments. Their robot functions similarly to the robotic system previously discussed in terms of the method for SMA actuation by heating up the opposing set of springs to actuate the end effector left and right. However, their system features an integrated water-cooling module that accelerates the cooling process. This is done by using water cooling to cool the springs and then introducing compressed air to quickly push the water out, expediting the next actuation cycle. Their setup is shown in Fig. 6 [40]. MRI compatibility was tested and after obtaining images before and actuation of the robot, there was only a 0.8% reduction in SNR. The stiffness of their robot was tested in order to conclude whether it can actuate through the SMA springs in a surgical environment. Their results obtained concluded that the stiffness of the SMA backbone was  $1.1 \times 10^{-4} N/m$ , which is an adequate resistivity force between the robot and most surgical environments.

After reviewing publications for each actuator, it can be seen that SMA actuation is one of the more favorable actuation methods for MRI-compatible robotic surgery due to the low SNR loss, high output, negligible limitation, and overall has less weaknesses compared to the other actuation methods as discussed in each actuation section. Performance of SMA versus other actuation methods is comparable in terms of SNR loss and system performance, which is an important characteristic of MRI-compatible robotic systems.

#### IV. CONCLUSION

Recently, SMA has slowly developed to be able to be integrated in MR-guided surgical interventions by fixing its main limitation of a cooling system for fast actuation. Throughout this paper, it has been identified that most robots designed for surgical applications rely a lot on its compatibility in MR settings with respect to meeting the SNR standards, as well as the overall performance of the robot in terms of speed and power. Costs and feasibility in all clinical settings also play a factor when selecting the type of MRI-compatible actuator. Despite the issues outlined in the articles that featured the four different actuation methods, actuators such as hydraulic and pneumatic still remain to be frequently used due to their overall performance. However, most workarounds with their outstanding issues tend to be inconvenient in most clinical settings that would require a lot of maintenance on the complex robotic systems. For example, not all clinical settings feature large areas to set up the hydraulic/pneumatic actuation systems with their long transmission lines and the need for a control room. It has also been shown that these recent robotic systems still require workarounds to function at an acceptable performance and feature a form of limitation, which will likely always be the case. Although SMA is characterized by slow natural response times, a recent application of this has implemented a

new cooling system that allows it to reach the same overall performance without having to overcome any significant obstacles that would either be too complicated or costly. Overall, it is a different approach that possesses the same, if not more advantages over the other popular actuation methods. Future research and attention towards implementing SMA would be a step in the right direction towards a more efficient method that produces similar results as the other actuation methods.

## REFERENCES

- [1] K. Mohiuddin and S. J. Swanson, "Maximizing the benefit of minimally invasive surgery," *Journal of surgical oncology*, vol. 108, no. 5, pp. 315–319, 2013.
- [2] T. Haidegger, S. Speidel, D. Stoyanov, and R. M. Satava, "Robotassisted minimally invasive surgery—surgical robotics in the data age," *Proceedings of the IEEE*, vol. 110, no. 7, pp. 835–846, 2022.
- [3] R. H. Caverly, "Mri fundamentals: Rf aspects of magnetic resonance imaging (mri)," *IEEE Microwave Magazine*, vol. 16, no. 6, pp. 20–33, 2015.
- [4] H. Su, K.-W. Kwok, K. Cleary, I. Iordachita, M. C. Cavusoglu, J. P. Desai, and G. S. Fischer, "State of the art and future opportunities in mri-guided robot-assisted surgery and interventions," *Proceedings of the IEEE*, 2022.
- [5] M. J. Winder, J. Spooler, and M. R. Mayberg, "The evolution of intraoperative imaging and neuro-navigation in transphenoidal surgery," *Journal of Surgical Radiology*, vol. 2, no. 1, 2011.
- [6] G. Li, H. Su, G. A. Cole, W. Shang, K. Harrington, A. Camilo, J. G. Pilitsis, and G. S. Fischer, "Robotic system for mri-guided stereotactic neurosurgery," *IEEE transactions on biomedical engineering*, vol. 62, no. 4, pp. 1077–1088, 2014.
- [7] T. Woods, "Guidance for industry and fda staff: Establishing safety and compatibility of passive implants in the magnetic resonance (mr) environment," *US Department of Health and Human Services, Food and Drug Administration*, vol. 21, 2008.
- [8] M. U. Farooq and S. Y. Ko, "A decade of mri compatible robots: Systematic review," *IEEE Transactions on Robotics*, 2022.
- [9] M. Roshanfar, J. Dargahi, and A. Hooshlar, "Toward semi-autonomous stiffness adaptation of pneumatic soft robots: Modeling and validation," in *2021 IEEE International Conference on Autonomous Systems (ICAS)*. IEEE, 2021, pp. 1–5.
- [10] H. Liang and Z. T. H. Tse, "Mr conditional prostate intervention systems and actuators review," *Proceedings of the Institution of Mechanical Engineers, Part H: Journal of Engineering in Medicine*, p. 09544119221136169, 2022.
- [11] D. J. S. Ruth, J.-W. Sohn, K. Dhanalakshmi, and S.-B. Choi, "Control aspects of shape memory alloys in robotics applications: A review over the last decade," *Sensors*, vol. 22, no. 13, p. 4860, 2022.
- [12] A. Hooshlar, S. Najarian, and J. Dargahi, "Haptic telerobotic cardiovascular intervention: a review of approaches, methods, and future perspectives," *IEEE reviews in biomedical engineering*, vol. 13, pp. 32–50, 2019.
- [13] A. Hooshlar, "Image-based force estimation and haptic rendering for robot-assisted cardiovascular intervention," Ph.D. dissertation, Concordia University, 2021.
- [14] T. Torkaman, M. Roshanfar, J. Dargahi, and A. Hooshlar, "Analytical modeling and experimental validation of a gelatin-based shape sensor for soft robots," in *2022 International Symposium on Medical Robotics (ISMR)*. IEEE, 2022, pp. 1–7.
- [15] N. Bandari, J. Dargahi, and M. Packirisamy, "Tactile sensors for minimally invasive surgery: A review of the state-of-the-art, applications, and perspectives," *Ieee Access*, vol. 8, pp. 7682–7708, 2019.
- [16] Z. Guo, Z. Dong, K.-H. Lee, C. L. Cheung, H.-C. Fu, J. D. Ho, H. He, W.-S. Poon, D. T.-M. Chan, and K.-W. Kwok, "Compact design of a hydraulic driving robot for intraoperative mri-guided bilateral stereotactic neurosurgery," *IEEE Robotics and Automation Letters*, vol. 3, no. 3, pp. 2515–2522, 2018.
- [17] S.-E. Song, N. B. Cho, G. Fischer, N. Hata, C. Tempany, G. Fichtinger, and I. Iordachita, "Development of a pneumatic robot for mri-guided transperineal prostate biopsy and brachytherapy: New approaches," in *2010 IEEE International Conference on Robotics and Automation*. IEEE, 2010, pp. 2580–2585.
- [18] H. Su, M. Zervas, G. A. Cole, C. Furlong, and G. S. Fischer, "Realtime mri-guided needle placement robot with integrated fiber optic force sensing," in *2011 IEEE International Conference on Robotics and Automation*. IEEE, 2011, pp. 1583–1588.
- [19] A. J. Taylor, T. Slutzky, L. Feuerman, H. Ren, J. Tokuda, K. Nilsson, and Z. T. H. Tse, "Mr-conditional sma-based origami joint," *IEEE/ASME Transactions on Mechatronics*, vol. 24, no. 2, pp. 883–888, 2019.
- [20] B. Yang, U.-X. Tan, A. B. McMillan, R. Gullapalli, and J. P. Desai, "Design and control of a 1-dof mri-compatible pneumatically actuated robot with long transmission lines," *IEEE/ASME transactions on mechatronics*, vol. 16, no. 6, pp. 1040–1048, 2010.
- [21] P. Shokrollahi, J. M. Drake, and A. A. Goldenberg, "A study on observed ultrasonic motor-induced magnetic resonance imaging (mri) artifacts," *biomedical journal*, vol. 42, no. 2, pp. 116–123, 2019.
- [22] S. S. Cheng, Y. Kim, and J. P. Desai, "New actuation mechanism for actively cooled sma springs in a neurosurgical robot," *IEEE Transactions on Robotics*, vol. 33, no. 4, pp. 986–993, 2017.
- [23] B. Murphy, P. L. Carson, J. H. Ellis, Y. Zhang, R. J. Hyde, and T. L. Chenevert, "Signal-to-noise measures for magnetic resonance imagers," *Magnetic Resonance Imaging*, vol. 11, no. 3, pp. 425–428, 1993.
- [24] P. Fekri, H. R. Nourani, M. Razban, J. Dargahi, M. Zadeh, and A. Arshi, "A deep learning force estimator system for intracardiac catheters," in *2021 IEEE International Symposium on Medical Measurements and Applications (MeMeA)*. IEEE, 2021, pp. 1–6.
- [25] M. Roshanfar, A. Sayadi, J. Dargahi, and A. Hooshlar, "Stiffness adaptation of a hybrid soft surgical robot for improved safety in interventional surgery," in *2022 44th Annual International Conference of the IEEE Engineering in Medicine & Biology Society (EMBC)*. IEEE, 2022, pp. 4853–4859.

- [26] A. Hooshiar, A. Sayadi, M. Jolaei, and J. Dargahi, "Analytical tip force estimation on tendon-driven catheters through inverse solution of cosserat rod model," in 2021 IEEE/RSJ International Conference on Intelligent Robots and Systems (IROS). IEEE, 2021, pp. 1829–1834.
- [27] A. Ameri, A. Molaei, M. A. Khosravi, A. G. Aghdamp, and J. Dargahi, "Modeling and control of cable-driven parallel robots with non-affine dynamics," in 2021 60th IEEE Conference on Decision and Control (CDC). IEEE, 2021, pp. 5582–5587.
- [28] P. Fekri, H. Khodashenas, K. Lachapelle, R. Cecere, M. Zadeh, and J. Dargahi, "Y-net: A deep convolutional architecture for 3d estimation of contact forces in intracardiac catheters," *IEEE Robotics and Automation Letters*, vol. 7, no. 2, pp. 3592–3599, 2022.
- [29] A. Molaei, A. G. Aghdam, and J. Dargahi, "A versatile pseudo-rigid body modeling method," *arXiv preprint arXiv:2206.06237*, 2022.
- [30] M. Jolaeimoghaddam, S. A. H. Ahmedi, and J. Dargahi, "Sensor-free force and position control of tendon-driven catheters through interaction modeling," Jul. 14 2022, *uS Patent App. 17/647,673*.
- [31] W. Zhao, Y. Zhang, and N. Wang, "Soft robotics: Research, challenges, and prospects," *Journal of Robotics and Mechatronics*, vol. 33, no. 1, pp. 45–68, 2021.
- [32] K.-H. Lee, K. C. D. Fu, Z. Guo, Z. Dong, M. C. Leong, C.-L. Cheung, A. P.-W. Lee, W. Luk, and K.-W. Kwok, "Mr safe robotic manipulator for mri-guided intracardiac catheterization," *IEEE/ASME Transactions on Mechatronics*, vol. 23, no. 2, pp. 586–595, 2018.
- [33] Z. Dong, Z. Guo, K.-H. Lee, G. Fang, W. L. Tang, H.-C. Chang, D. T. M. Chan, and K.-W. Kwok, "High-performance continuous hydraulic motor for mr safe robotic teleoperation," *IEEE Robotics and Automation Letters*, vol. 4, no. 2, pp. 1964–1971, 2019.
- [34] D. Navarro-Alarcon, S. Singh, T. Zhang, H. L. Chung, K. W. Ng, M. K. Chow, and Y. Liu, "Developing a compact robotic needle driver for mri-guided breast biopsy in tight environments," *IEEE Robotics and Automation Letters*, vol. 2, no. 3, pp. 1648–1655, 2017.
- [35] Y. Chen, A. Squires, R. Seifabadi, S. Xu, H. K. Agarwal, M. Bernardo, P. A. Pinto, P. Choyke, B. Wood, and Z. T. H. Tse, "Robotic system for mri-guided focal laser ablation in the prostate," *IEEE/ASME Transactions on Mechatronics*, vol. 22, no. 1, pp. 107–114, 2016.
- [36] A. Krieger, S.-E. Song, N. B. Cho, I. I. Iordachita, P. Guion, G. Fichtinger, and L. L. Whitcomb, "Development and evaluation of an actuated mri-compatible robotic system for mri-guided prostate intervention," *IEEE/ASME Transactions on Mechatronics*, vol. 18, no. 1, pp. 273–284, 2011.
- [37] Y. Shi, N. Li, C. C. Tremblay, and S. Martel, "A piezoelectric robotic system for MRI targeting assessments of therapeutics during dipole field navigation," *IEEE/ASME Transactions on Mechatronics*, vol. 26, no. 1, pp. 214–225, 2020.
- [38] M. Runciman, A. Darzi, and G. P. Mylonas, "Soft robotics in minimally invasive surgery," *Soft robotics*, vol. 6, no. 4, pp. 423–443, 2019.
- [39] S. Shao, B. Sun, Q. Ding, W. Yan, W. Zheng, K. Yan, Y. Hong, and S. S. Cheng, "Design, modeling, and control of a compact sma-actuated mr-conditional steerable neurosurgical robot," *IEEE Robotics and Automation Letters*, vol. 5, no. 2, pp. 1381–1388, 2020.
- [40] Y. Kim, S. S. Cheng, and J. P. Desai, "Active stiffness tuning of a springbased continuum robot for mri-guided neurosurgery," *IEEE Transactions on Robotics*, vol. 34, no. 1, pp. 18–28, 2017.